ISTITUTO NAZIONALE FISICA NUCLEARE

INFN/BE - 73/2
20 Giugno 1973

F. Demanins, L. Granata, G. Nardelli and G. Pauli

ELASTIC SCATTERING OF FAST NEUTRONS BY ^{6}Li AND ^{12}C BETWEEN 1,98 MeV AND 4,64 MeV

ELASTIC SCATTERING OF FAST NEUTRONS BY ^{6}Li AND ^{12}C BETWEEN 1,98 MeV AND 4,64 MeV.

F. Demanins, L. Granata and G. Pauli

Istituto di Fisica, Università di Trieste and Istituto Nazionale Fisica Nucleare - Sezione di Trieste

G. Nardelli

Istituto di Fisica, Università di Padova and Istituto Nazionale Fisica Nucleare - Sezione di Padova

S U M M A R Y

A measurement of the angular distribution of neutrons scattered from ^{6}Li and ^{12}C at eight energies between 1,98 MeV and 4,64 MeV is described.

The differential cross-section deduced from the measured angular distribution are reported and compared with the data given by other authors. A comparison is made also with the results of a calculation based on the optical model with two potentials, i.e., the Perey-Buck and the gaussian potentials.

Also described is the neutron spectrometer with two detection channels, which has been used for the experiment.

INTRODUCTION

This report describes the methods and the results of an experimental study of the scattering of the fast neutrons from ^{6}Li and ^{12}C, which was undertaken in the effort of providing information on the differential cross-sections with a precision sufficient for their use in applied neutron physics and for a comparison with the results of calculations based upon the optical model.

The experimental data of this work belong to a series of data obtained in the course of measurements performed to test and calibrate a time-of-flight spectrometer for neutrons, capable of making simultaneous measurements at two scattering angles, realized for studying neutron emitting reactions.

With this apparatus, the angular distributions of the neutrons scattered by the nuclei ^{6}Li and ^{12}C have been measured for eight values of the incident neutron energy in the interval from 1.98 MeV to 4.64 MeV. The angular distributions have been determined at thirteen angles in the interval from 30° to 140°, in the laboratory frame of reference. The differential and the total elastic cross-sections have been then deduced from the angular distributions.

Several experimental studies of the neutron scattering from ^{6}Li and ^{12}C have been published. A literature survey rather complete to 1972 is reported in CINDA 72 (Ref. 1).

The differential and the total elastic cross-sections obtained in the present work are here compared with the data given by other authors. The differential and the total elastic cross-sections for ^{6}Li are compared with those given by Batchelor et al.([2]) for incident neutrons energies of 3.35- and 4- MeV, and with those given by Hopkins et al.([3]) for 4.83 MeV. The differential and the total elastic cross-section for ^{12}C are compared with the results given by Wills et al.([4]) for incident neutron energies of 2.02-, 2.28-, 2.51-, 2.76-, 4.10- MeV, Lane et al. ([5]) for 2.28 MeV, Walt et al.([6]) for 4.10 MeV, Perey ([7]) for 4.6 MeV, Budde et al.([8]) for 3.20 MeV and Galati et al.([30]) for 3.20-, 4.10-, 4.64 MeV. The total elastic cross-sections for ^{12}C are also compared with the data of Cierjaks et al.([9]), Lister et al.([10]), Metellini ([11]), Glasgow et al.([12]), Bockelman et al.([13]) and Boschung et al.([14]).

EXPERIMENTAL METHOD

The measurements described herewith have been carried out by employing the fast-neutron pulsed-beam time-of-flight technique. The apparatus consisted of the 5.5 MeV pulsed Van de Graaff accelerator of the "Laboratori Nazionali dell' INFN di Legnaro" and a two-angle detector system capable of making simultaneous time-of-flight measurements at two scattering angles. Pulsed beams of deuterons and protons having a repetition frequency of 3 MHz and a pulse length of 2 ÷ 3 ns have been used. During the measurements, the particle beams were analysed in momentum with the aid of a 90° deflection magnet and defined in energy to 0.1% by means of collimators.

Neutrons were produced by means of the $T(p,n)^3He$ and $D(d,n)^3He$ reactions, using targets of tritium adsorbed in titanium in the first case and targets of deuterium adsorbed in titanium in the latter case. For the experiments, the scattering samples were submitted to bombardament of neutrons emitted at 0° with respect to the charged particle beam direction and having energies E_n of 1.98-, 2.24-, 2.49-, 2.74-, 2.98-, and 3.20- MeV in the case of the T+p reaction and 4.10- and 4.64- MeV in the case of the D+d reaction.

The scattering samples were right cylinders 2,5cm in diameter and 4 cm high. They were placed with their axis perpendicular to the incident neutron beam direction and at a distance of 10cm from the neutron source. The carbon sample was made of nuclear grade graphite; isotopic enrichment for the sample of ^6Li was 95,3% and the sample contained less than 2% of impurities, the major component being oxigen.

Both samples were enclosed in aluminium cans of 0.01 cm thickness and were kept in the neutron beam by means thin nylon threads. The background was measured using an emtpy aluminium can.

The two neutron detectors were placed on the two arms of a goniometer, whose axis was coincident with the axis of the scattering sample. Each detector was placed at a distance of 2 meters from the scattering samples. The detectors were sorrounded by cylindrical shields containing water and boric acid, and by paraffin and lead as is shown schematically in figure 1. The detectors were also shielded against the source neutrons by additional shields placed close to the target on the goniometer arms.

This detector system associated with the pulse neutron source de-

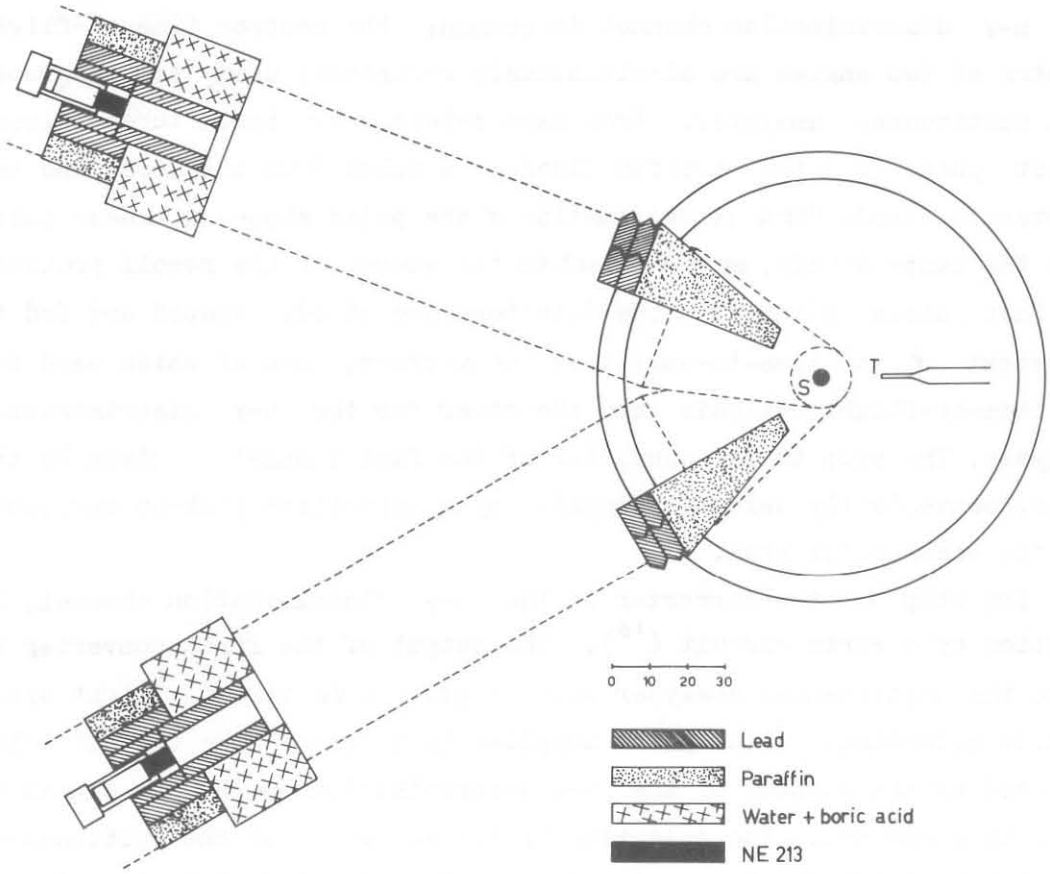

Fig. 1 - Arrangement of the spectrometers and of the shields with respect to the neutron source T and the scattering sample S, during the measurements.

scribed above realizes a time-of-flight spectrometer for neutrons. Figure 2 shows a block diagram of the electronics.

The neutron detectors are liquid scintillator (NE213) of cylindrical shape, 5 cm in diameter and 7.5 long, coupled to 56 AVP photomultipliers.

The neutron spectrometry is performed using the fast channel and the n-γ discrimination channel in common: the neutron time-of-flight spectra at two angles are simultaneously registered using two subgroups of a multichannel analyzer. From each detector are taken three pulses: a fast pulse from the twelfth dinode; a pulse from the anode and the fourteenth dinode for a discrimination of the pulse shape; a linear pulse from the tenth dinode, proportional to the energy of the recoil protons. The fast pulses coming from the detectors are mixed, shaped and fed to the start of two time-to-amplitude converters, one of which used for the time-of-flight analysis and the other for the n-γ discrimination analysis. The stop to the converter of the fast channel is given by the pulse, conveniently delayed, supplied by a capacitive pick-up surrounding the accelerator beam.

The stop to the converter of the n-γ discrimination channel, is supplied by a Forte circuit ([15]). The output of the first converter is fed to the multichannel analyzer which registers the time-of-flight spectrum, in coincidence with a pulse supplied by a coincidence circuit which is acted by the signals of the n-γ discrimination and by the signal of the linear channel. The selection of the subgroups of the multichannel analyser is performed by a signal taken from the discriminator of the linear channel "A". So, the registration of the events recorded by the two detectors, can be performed employing simultaneously two subgroups of channels while using for both detectors the same circuits for the spectrometry and for the n-γ discrimination. The low-energy cut-off of the detector system has been fixed by putting, after having excluded the n-γ discrimination, the threshold of the discriminators of the linear channels of the two detectors at the level of the highest pulses caused by the 59.6 keV gamma rays of the ^{241}Am. This corresponds for the neutrons to an energy threshold of 450 keV ([16]).

The level of the low-energy cut-off as well as the efficiency of the n-γ discrimination system have been frequently verified during the neutron scattering runs.

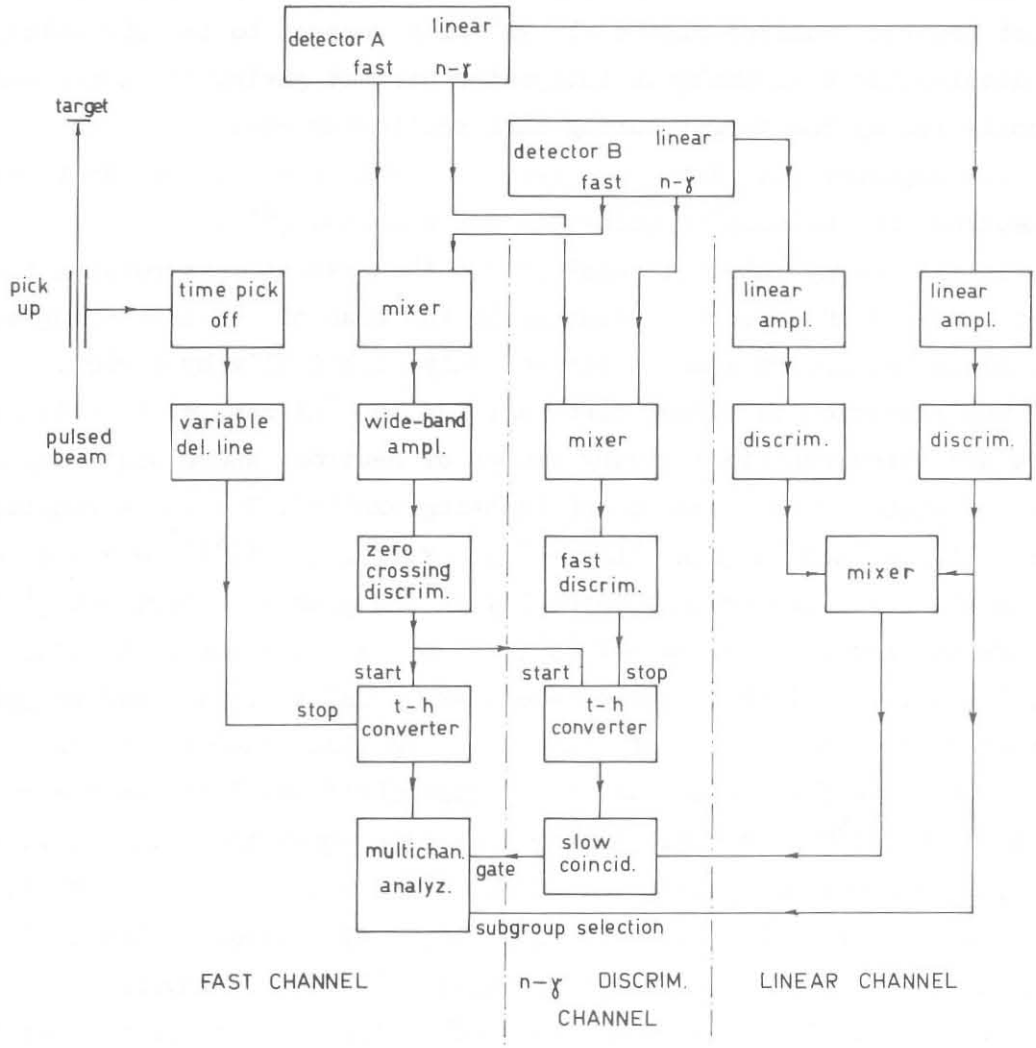

Fig. 2 - Block diagram of the electronics.

The efficiency of the detectors have been determined by measuring the neutron flux emitted at 0°in the $T(p,n)^3He$ and $D(d,n)^3He$ reactions, using the cross-sections reported in the literature ([17,18]) and by measuring the n-p elastic scattering.

The normalization of the experimental data was provided either by a fast neutron monitor placed at 90° with respect to the direction of the accelerator beam and by an integrator circuit giving the total charge collected by the target during each scattering run.

The experimental data have been corrected for multiple scattering of neutrons in the samples using the Cox's method ([29]).

In the energy interval considered in the present measurements there is no problem of energy resolution in the case of ^{12}C scattering sample, since the neutrons are scattered only elastically by carbon.

The situation is rather different for the ^6Li sample. In this case there are three reactions giving groups of neutrons whose width depends upon the width of the level which is being excited. The three reactions are: $^6Li(n,n)^6Li$; $^6Li(n,n')^6Li^* \rightarrow {}^6Li + \gamma$; $^6Li(n,n')^6Li^* \rightarrow \alpha + d$, and the levels which are brought into play in the present experiment ([19,20,21]) are the level at 2.184 MeV (3^+, T = 0) and the level at 3.560 MeV (0^+, T = 1). The width of these levels are equal to 25 ± 1 keV and 5keV respectively. In the case of ^6Li there are also other reactions which emit neutrons with a continuous energy distributions. There are the reactions $^6Li(n,d)^5He \rightarrow \alpha + n$, having a Q-value equal to -2.428 MeV, and $^6Li(n,dn')\alpha$ breaking-up into three bodies and having a Q-value of -1.471 MeV. One more reaction to be considered, which gives neutrons with a continuous energy spectrum, is the reaction $^6Li(n,2n)\alpha$ having a Q-value of -3.696 MeV. This reaction produces neutrons twice as much as the other reactions but the larger production is compensated by a lower cross-section than for the other reactions ([22]).

As an example of the data which were obtained with the spectrometer described above, in figure 3 is reported the spectrum measured with the ^6Li sample, for an incident neutron energy of 4.64 MeV and a scattering angle 30°in the laboratory reference system. In the same figure is also reported the background spectrum which was measured for an identical total amount of charge collected at the target. The structures of this spectrum are caused by the shields and collimators.

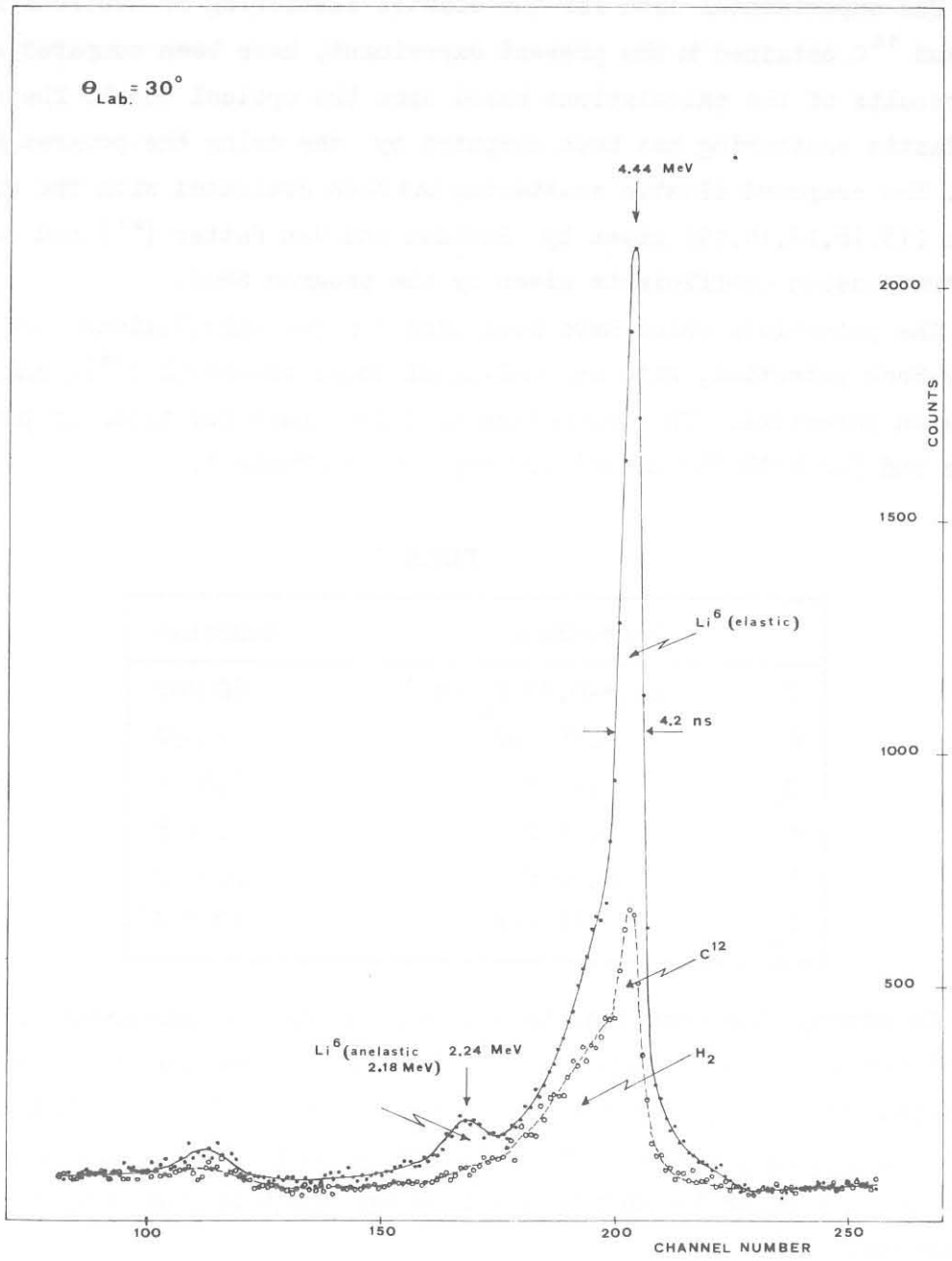

Fig. 3 - Time-of-flight spectrum of 4,64 MeV neutrons scattered at 30^{o} (lab) from ^{6}Li. The open circles refer to a background measurement.

COMPARISON WITH THE CALCULATED DATA

The experimental data for the elastic scattering of neutrons from ^{6}Li and ^{12}C obtained in the present experiment, have been compared with the results of the calculations based upon the optical model. The shape elastic scattering has been computed by the using the program SMOG ([23]). The compound elastic scattering has been evaluated with the equations (13,16,17,18,19) given by Sheldon and Van Patter ([24]) and using the trasmission coefficients given by the program SMOG.

The potentials which have been used in the calculations are the Perey-Buck potential, with an equivalent local potential ([25]), and the gaussian potential. The parameters used for these two types of potentials and for both the nuclei are reported in Table 1.

TABLE 1

	Perey-Buck	Gaussian
V	49,3-0,33 E_n(MeV)	50 MeV
W	5,75 MeV	7 MeV
r_o	1,25 f	1,25 f
a	0,65 f	0,65 f
b	0,70 f	0,98 f
V_S	11 MeV	19 MeV

No attempt has been done in order to improve the agreement between experimental and calculated data by varying the parameters of two potentials. The reason for this is that the nature of the nuclei which are investigated and the range of energies considered in the measurements do not allow to obtain a better agreement by just varying such parameters.

RESULTS

The angular distributions of the neutrons elastically scattered by ^{6}Li are shown in figure 4 for the incident neutron energies of 1.98-, 2.24-, 2.49-, 2.74- MeV, and in fig.5 for 2.98-, 3.20-, 4.10- and 4.64- MeV.

For the sake of comparison, in fig. 5, at 3.20- and 4.10 MeV, are

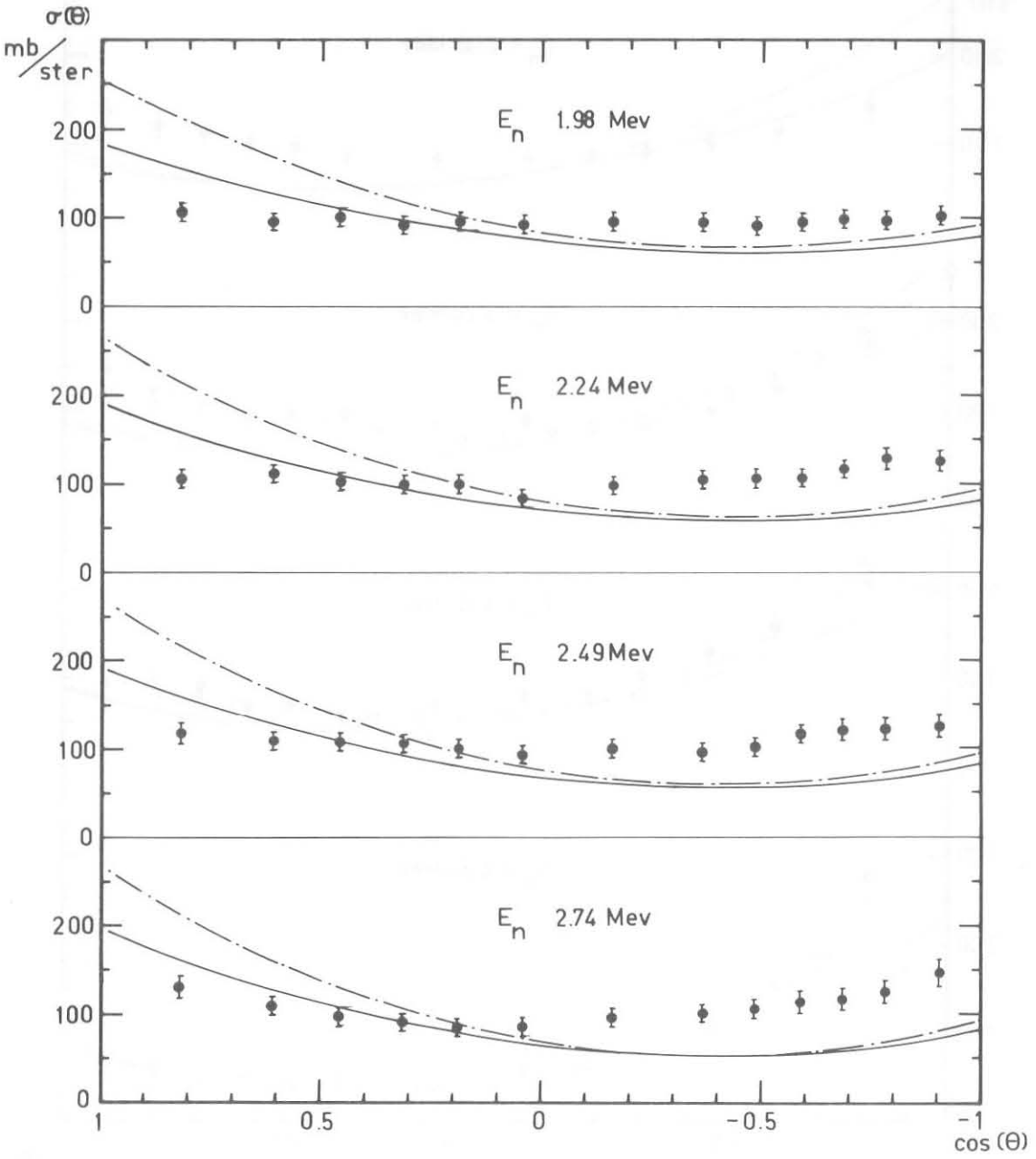

Fig. 4 - Angular distributions of neutrons elastically scattered from ^{6}Li:

● experimental data

—— curve calculated with the optical model and the gaussian potential

·—· curve calculated with the optical model and the Perey-Buck potential

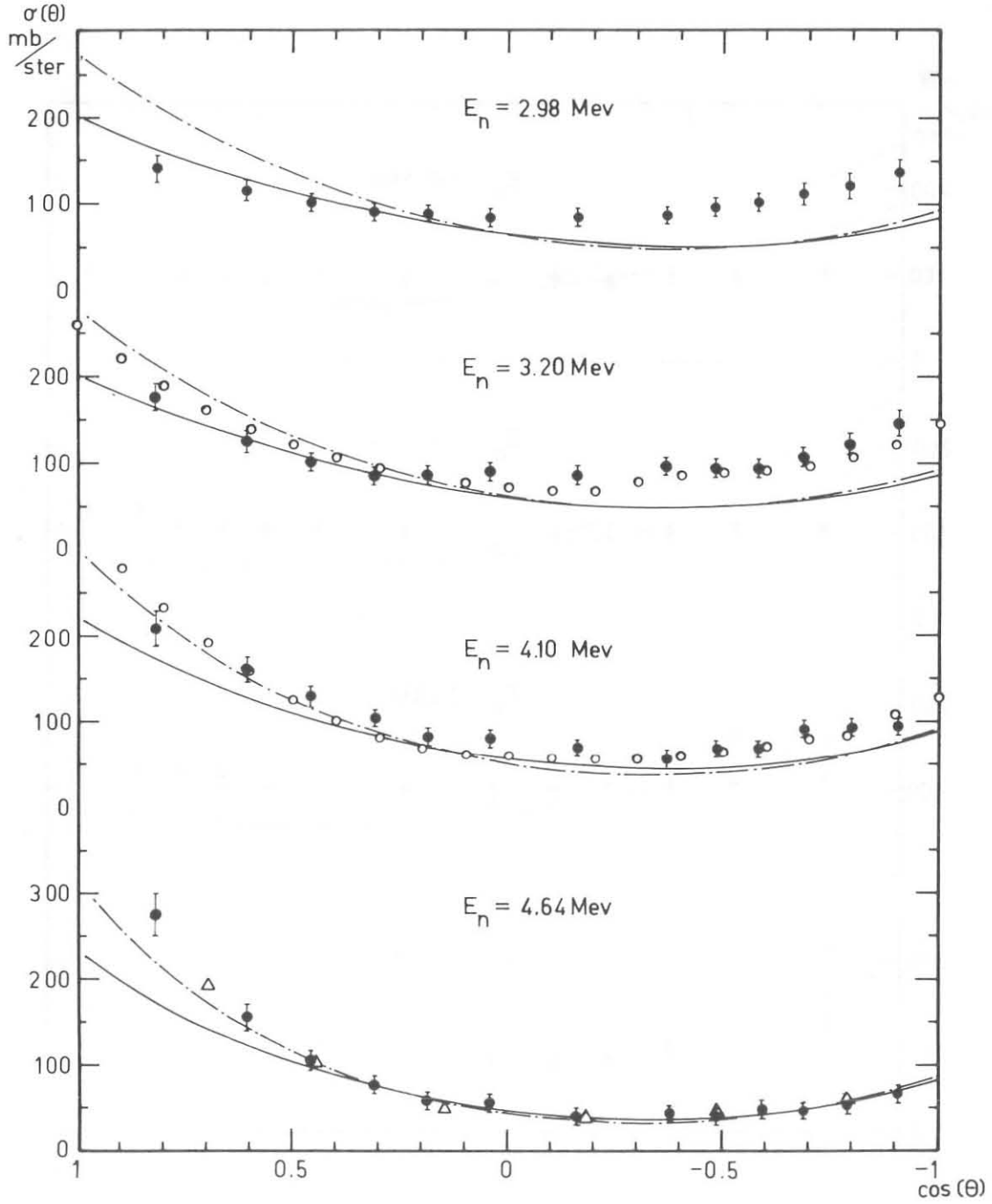

Fig. 5 - Angular distributions of neutrons elastically scattered by ^{6}Li:

● present work

○ Batchelor and Towle (Ref. 2)

△ Hopkins and Drake (Ref. 3)

—— optical model and gaussian potential

·—·—· optical model and Perey-Buck potential.

shown the data obtained by Batchelor and Towle ([2]) through a best fit of the experimental data at 3.35- and 4.0 MeV respectively. Since in the energy range which is considered there are no resonance structures in the total elastic cross-section, as can be seen by inspecting fig. 6, the agreement is satisfactory in spite of the energies not being quite the same. A comparison is also made between the data for 4.64 MeV and the data of Hopkins and Drake ([3]) for 4.83 MeV.

In fig.3 and 4 are also shown the differential cross-sections obtained with the potentials and the optical model calculations described in previous paragraph. The values of the differential cross-sections are listed in table 2: the data are given for the thirteen angles and for the eight energies at which the measurements have been carried out. In the same table are also reported the total elastic cross-sections deduced from such data.

The total elastic cross-sections is displayed in fig.6 as a function of energy; the data obtained in the present work are compared with the data of the authors previously mentioned and with the data predicted by the optical model calculations for the two potentials.

In figs.7,8 and 9 are shown the angular distributions of the neutrons elastically scattered by ^{12}C for the incident neutron energies of 1.98-, 2.24- and 2.49 MeV; 2.74-, 2.98- and 3.20 MeV; 4.10- and 4.64 MeV respectively. In the figures, together those obtained with the optical model are reported the differential cross-sections obtained in a previous work ([26]) which was concerned with a phase-shift analysis of the experimental data reported in this report.

Also in the case of carbon the results of the present work are compared with the results obtained by other authors at the same energies or at slight different energies:
the data at 1.98 MeV are compared with the data of Wills et al. ([4]) at 2.02 MeV; the data at 2.24 MeV with those of Wills et al. at 2.28 and with those of Lane et al. ([5]) at 2.242 MeV; the data at 2.49 MeV and 2.74 MeV with those of Wills et al. at 2.51 MeV and 2.76 MeV; the data at 3.20 MeV with those at 3.20 MeV of Galati et al. ([30]) and of Budde and Huber ([8]); the data at 4.10 MeV with those at 4.10 MeV of Wills et al. and of Walt and Beyster ([6]), and with those of Galati et al. at 4.075 MeV; the data at 4.64 MeV with those of Galati et al. at 4.64 and

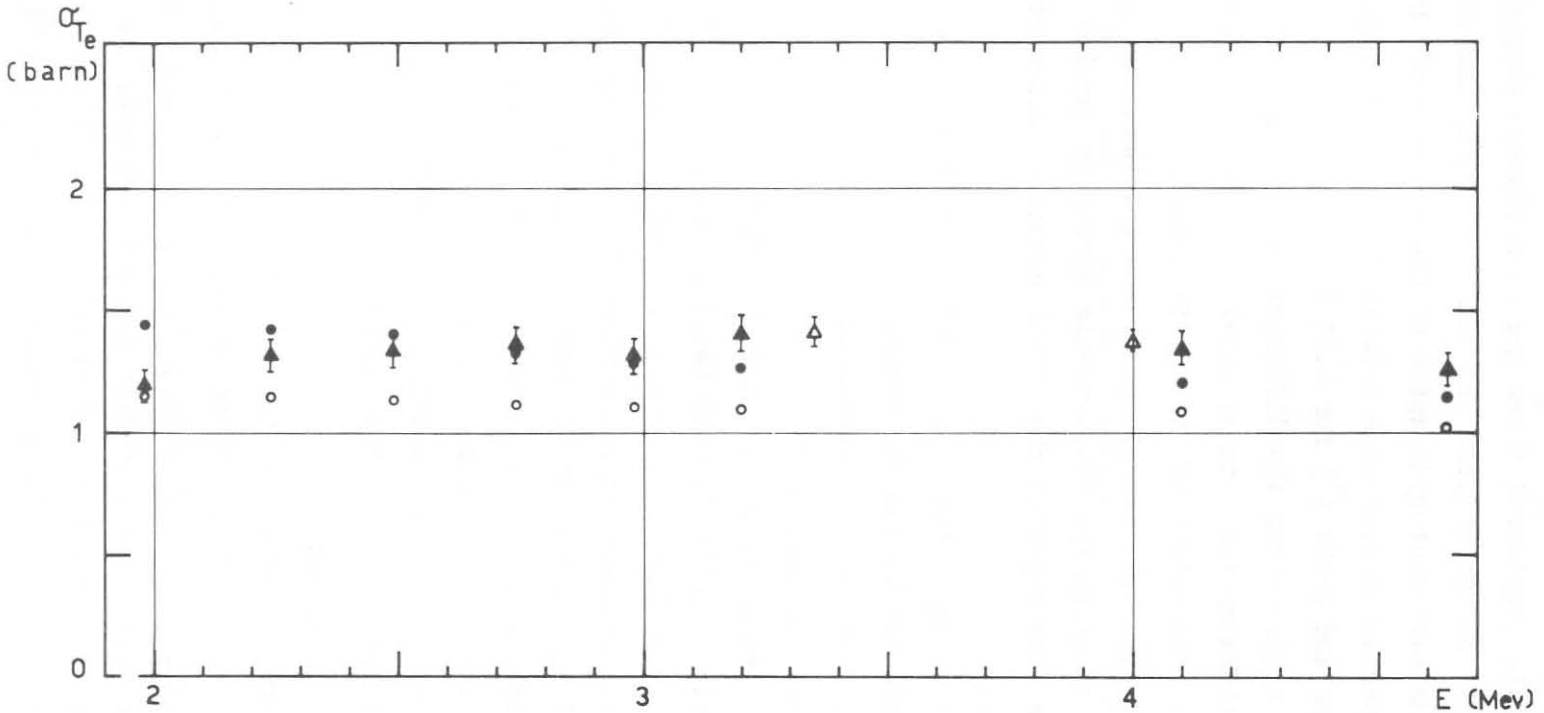

Fig. 6 - The total elastic cross section of neutrons for ^{6}Li plotted as a function of energy:

▲ this experiment

△ Batchelor and Towle (Ref. 2)

○ optical model and gaussian potential

● optical model and Perey-Buck potential

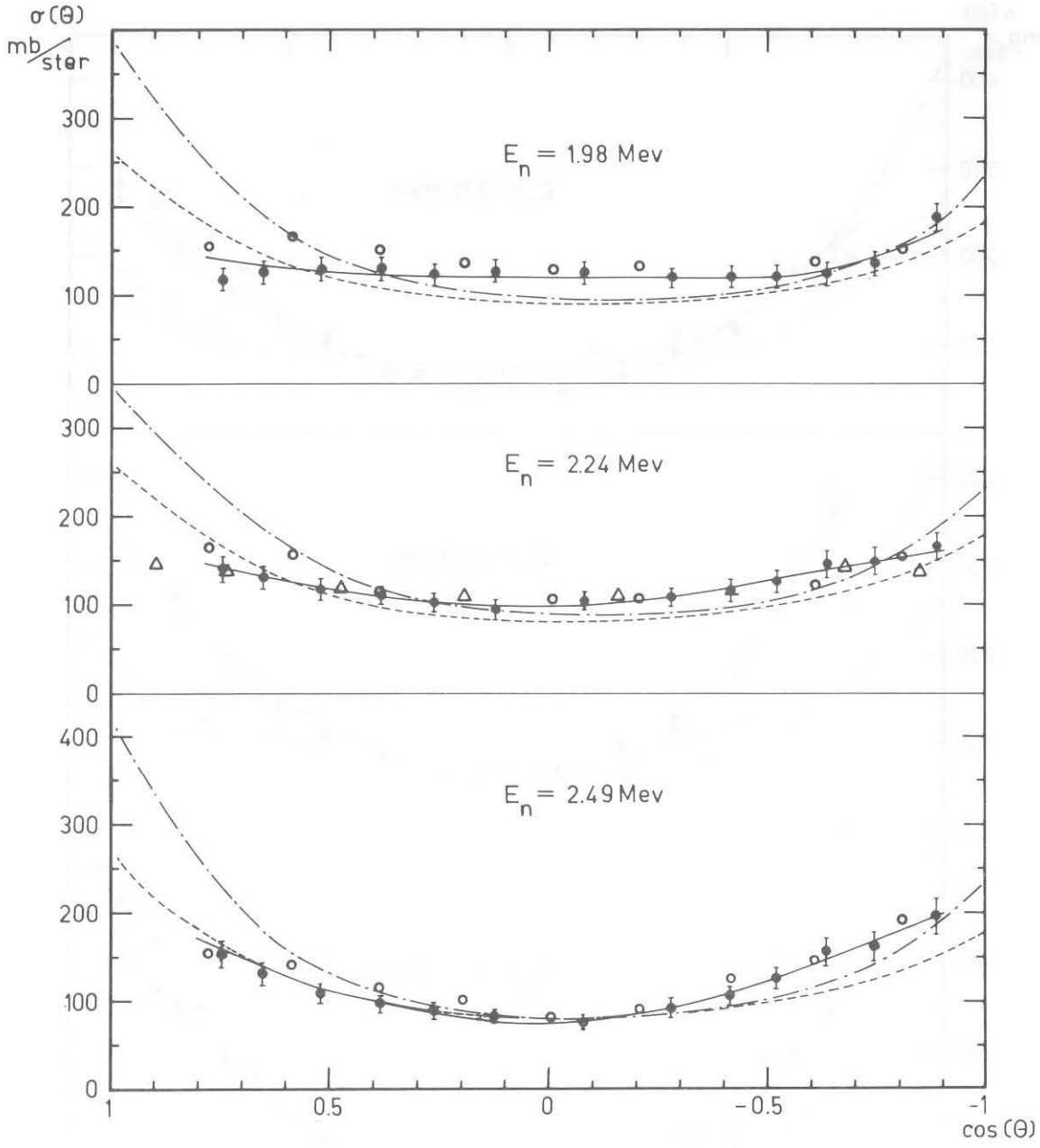

Fig. 7 - Angular distributions of the neutrons elastically scattered by ^{12}C:

- ● this experiment
- ○ Wills et al. (Ref. 4)
- △ Lane et al. (Ref. 5)
- —— angular distributions deduced from a phase-shift analysis (Ref. 26)
- ---- optical model and gaussian potential
- ·—·— optical model and Perey-Buck potential

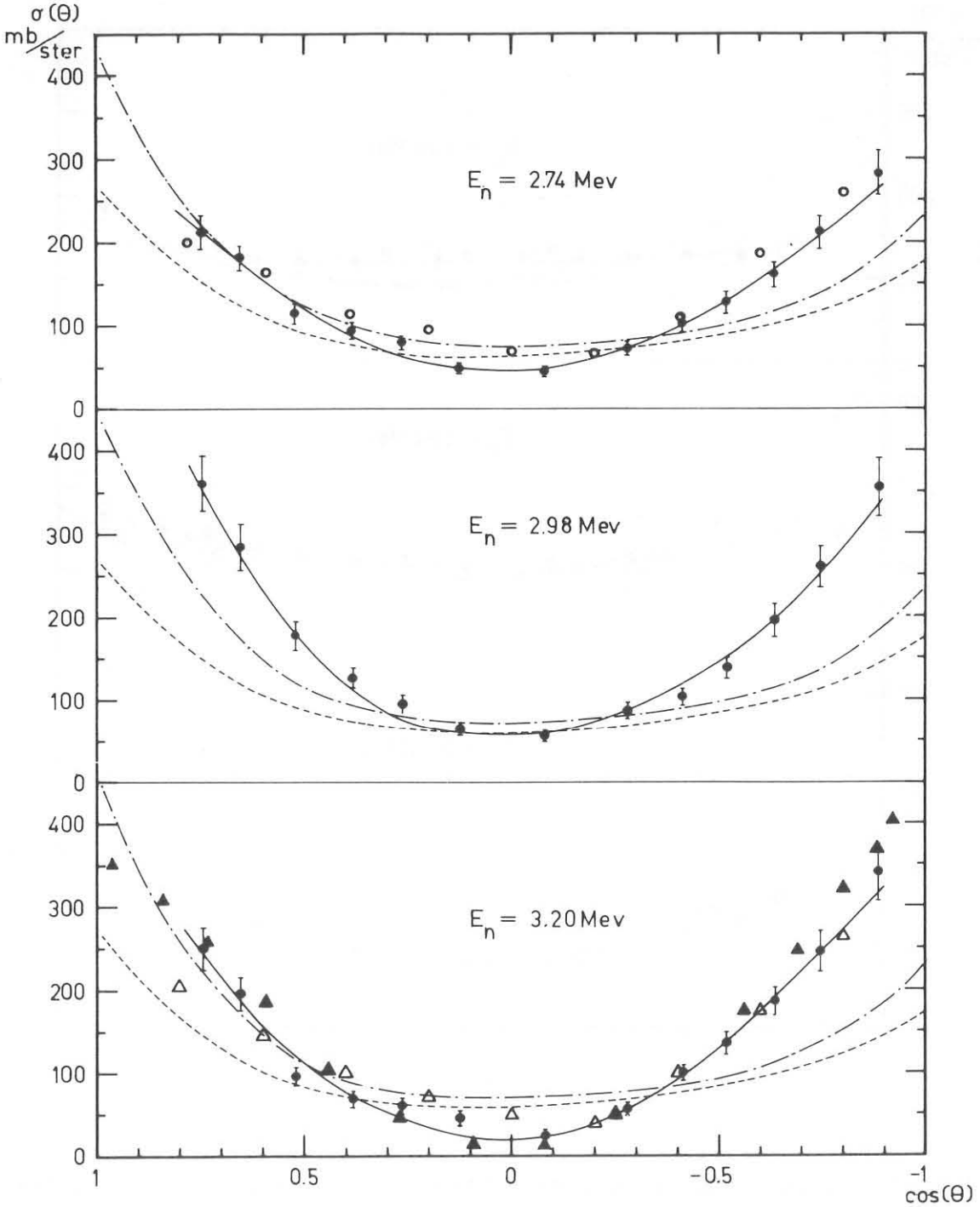

Fig. 8 - Angular distributions of the neutrons elastically scattered by ^{12}C:

● this experiment, ○ Wills et al. (Ref. 4)

△ Budde and Huber (Ref. 8), ▲ Galati et al. (Ref. 30)

—— angular distributions deduced from a phase-shift analysis (Ref. 26)

– – – optical model and gaussian potential

·—·—· optical model and Perey-Buck potential

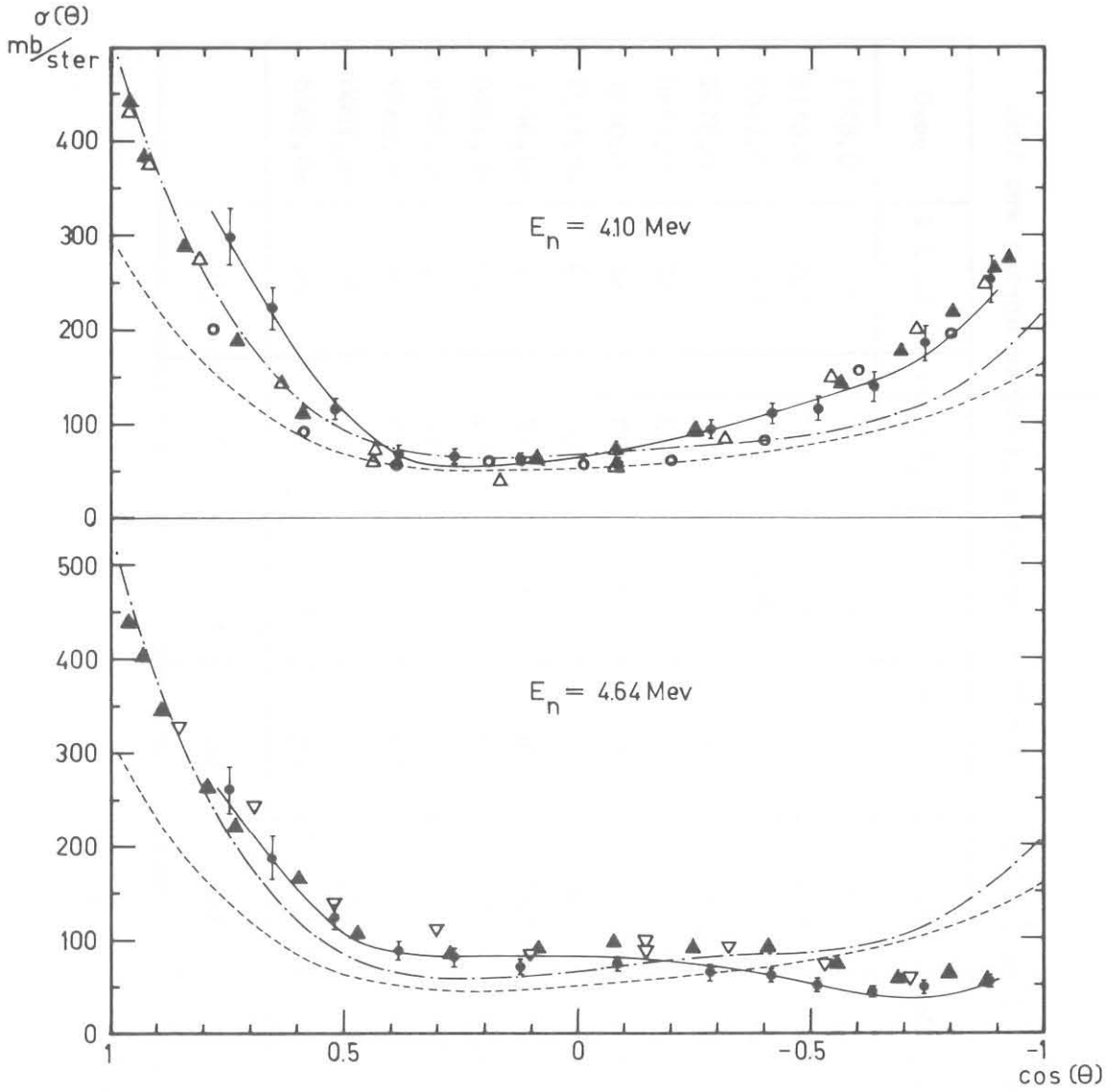

Fig. 9 - Angular distributions of the neutrons elastically scattered by ^{12}C:

- ● this experiment
- ○ Wills et al (Ref. 4)
- △ Walt and Beyster (Ref. 6)
- ▽ Perey (Ref. 7)
- ▲ Galati (Ref. 30)
- —— phase shift analysis
- – – – optical model and gaussian potential
- ·—·—· optical model and Perey-Buck potential

TABLE 2 - Differential elastic cross-section (mb/ster) for ^{6}Li, estimated absolute errors are 10%.

$\Theta_{C.M.}$	1,98 MeV	2,24 MeV	2,49 MeV	2,74 MeV	2,98 MeV	3,20 MeV	4,10 MeV	4,64 MeV	cosΘ
34°48′	101	106	114	130	141	178	208	274	0,8211
52°18′	96	111	108	109	113	125	161	155	0,6115
62°34′	99	101	106	98	100	100	128	104	0,4607
71°34′	90	97	104	90	90	85	102	75	0,3162
79°10′	94	98	99	86	87	85	80	57	0,1880
87°25′	92	82	91	87	82	89	80	54	0,0451
99°38′	94	98	98	96	83	85	68	39	-0,1673
111°25′	94	103	94	100	86	94	57	42	-0,3651
119°	89	106	100	105	96	93	68	40	-0,4848
125°34′	93	104	115	112	101	93	67	47	-0,5816
133° 8′	97	116	118	116	111	105	89	46	-0,6837
141°20′	96	128	121	124	121	121	83	54	-0,7808
154°48′	101	124	124	146	135	145	95	66	-0,9048
$\sigma_{Te}^{(a)}$	1197	1321	1334	1364	1311	1406	1338	1254	

(a) Total elastic cross-section (mb)

TABLE 3 - Differential elastic cross-sections (mb/ster) for ^{12}C. Estimate absolute errors are 10%

$\Theta_{C.M.}$	1,98 MeV	2,24 MeV	2,49 MeV	2,74 MeV	2,98 MeV	3,20 MeV	4,10 MeV	4,64 MeV	$\cos\Theta$
32°24′	117	140	152	212	361	251	297	261	0,8443
48°55′	124	131	131	182	283	195	222	188	0,6572
58°40′	129	117	108	115	178	96	115	124	0,5200
67°17′	130	110	96	94	125	67	68	89	0,3862
74°37′	122	100	89	79	95	59	67	79	0,2653
82°41′	127	93	82	48	65	44	62	70	0,1274
94°48′	125	103	76	46	55	23	56	72	-0,0837
106°41′	118	108	92	72	85	55	92	62	-0,2871
114°25′	119	116	106	99	104	99	110	59	-0,4134
121°16′	118	123	124	127	138	134	116	49	-0,5190
129°10′	123	145	156	160	195	183	138	42	-0,6316
137°55′	134	147	161	212	260	245	184	48	-0,7422
152°24′	174	164	195	282	356	340	253	54	-0,8862
$\sigma_{Te}^{(a)}$	1671	1533	1520	1659	2300	1734	1835	1307	

(a) Total elastic cross-sections (mb)

with those of Perey ([7]) at 4.6 MeV.

By inspecting the figs.3 to 9 one can see that the angular distributions obtained in the present work are in good agreement with those given by the other authors, within the errors ascribed to the measurements. The values of the differential elastic cross-sections and of the total elastic cross-sections for the case of carbon are listed in table 3.

The experimental data of the other authors, either for ^{6}Li and for ^{12}C, are reported in the figures without the errors in order to simplify the drawings.

The total cross-section for ^{12}C measured as a function of the incident neutron energy is displayed in fig. 10. The data obtained from the angular distributions of the present work are compared with the data given by Wills ([4]), by Cierjaks et al. ([9]), by Lister and Sayres ([10]), by Metellini ([11]), by Glasgow and Foster ([12]), by Bockelman et al. ([13]) and with the datum at 4.04 MeV given by Boschung et al. ([14]). The data of Cierjaks et al. were obtained by means of trasmission measurements performed with a continuous neutron spectrum and the time-of-flight method. In fig. 10 are not reported all the values obtained by the various authors but only those necessary to give the behaviour of the cross-section. Only for the two narrowest resonances at 2.077 MeV (Γ = 6 keV) and 2.82 MeV ($\Gamma \sim 5$ keV) (Ref. [27]) all the measured values are shown. The measured total cross-sections turn out to be larger than the total elastic cross-section, obtained in the present work and by other authors ([4])([10])([11])([12])([13]), over almost the entire energy range which has been considered. About this point, one can say that the total elastic cross-section, deduced from the angular distributions by extrapolating the data in the regions of small and large angles where there is lack of measurements, can result to be different from the measured total cross-sections. Anyway it has to be noticed the sistematic discrepancy in the range from 2 to 3 MeV. In this range, further investigations are necessary, including small and large angles, about the angular distributions of the elastically scattered neutrons. It is worthwhile to notice anyhow that the measurements of the total cross-section performed by Knowless and O'Dell ([28]), which covers also the energy range above mentioned, gave results smaller than those of Cier-

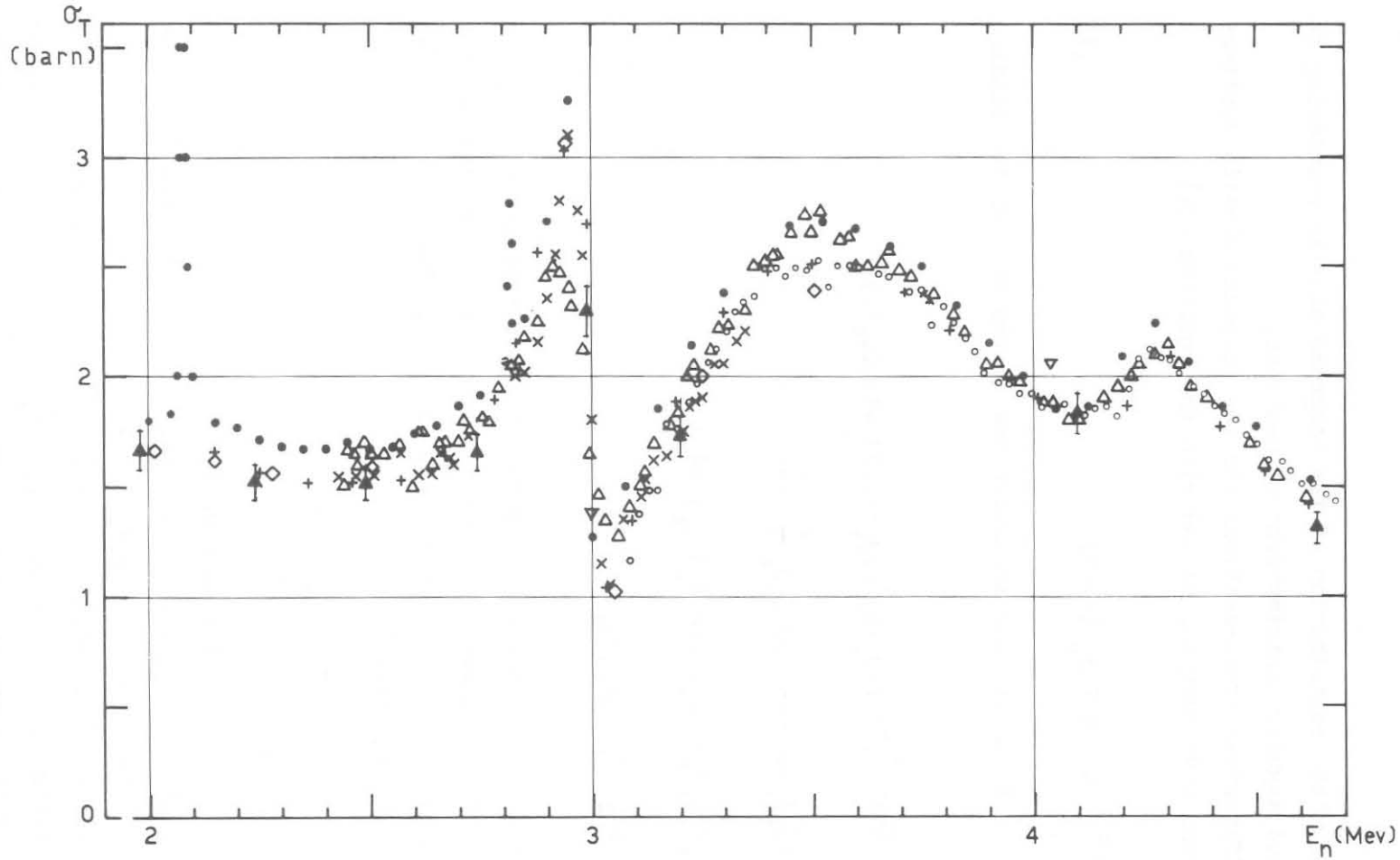

Fig. 10 - Total elastic cross section of neutrons for ^{12}C plotted as a function of energy:
▲ this experiment, ● Cierjaks et al. (Ref. 9) (see text)
○ Lister and Sayres (Ref. 10), + Metellini (Ref. 11)
△ Glasgow and Foster (Ref. 12), × Bockelman et al. (Ref. 13)
◇ Wills et al. (Ref. 4), ▽ Boschung et al. (Ref. 14).

jaks et al.. Such measurement was carried out with a Linac, and then with an extended neutron spectrum, and the time-of-flight technique.

Appendix

Determination of the contribution of the compound elastic scattering to the calculated angular distributions of neutrons.

The differential cross-sections for the compound elastic scattering of neutrons have been calculated with the equation (24)

$$\frac{d\delta}{d\Omega} = \frac{1}{8}\,\lambda^2 \sum N\ C\ W\ \tau\ P_\nu\ (\cos\Theta) \qquad (1)$$

The first three terms of the summation are in the case of the elastic scattering

$$N = (-1)^{2J_0-2J_1-1}\ (2J_1+1)^2(2j_1+1)(2j_2+1)(2J_0+1)^{-1}$$

$$C = \langle \nu 0 | j_1 j_1 \tfrac{1}{2} -\tfrac{1}{2} \rangle \langle \nu 0 | j_2 j_2 \tfrac{1}{2} -\tfrac{1}{2} \rangle$$

$$W = W(J_1 J_1 j_1 j_1 ; \nu J_0)\ W(J_1 J_1 j_2 j_2 ; \nu J_2)$$

with $\quad 0 \leq \nu \leq 2j_1 ; 2J_1 ; 2j_2$

where J_o is the spin of the ground level of the target nucleus, J_1 the spin of the compound nucleus, j_k and ℓ_k the spins and orbital angular moment of the entry (k=1) and exit (k=2) channels. The Hauser and Feshabach penetrability term is

$$\tau = T_{\ell_1}(E_1)\ T_{\ell_2}(E) \left[\sum_{\ell J E} T_\ell(E) \right]^{-1}$$

as a function of the trasmission coefficients.

This is valid in general and in particularly for the ^{6}Li whose transition is of the type $1^+ \rightarrow J_1 \pi_1 \rightarrow 1^+$.

In the case of ^{12}C, which is characterized by the transition $0^+ \rightarrow J_1 \pi_1 \rightarrow 0^+$, being equal the spins, $j_1 = J_1 = j_2$, and the orbital angular momentaof the entry and exit channels, $\ell_1 = \ell_2$, the first three terms of the summation in Eq. (1) become

$$N = (-1)^{2J_o - 2J_1 - 1} (2J_1 + 1)^4 (2J_o + 1)^{-1}$$

$$C = \left[\langle \nu 0 | J_1 J_1 \; \frac{1}{2} \; -\frac{1}{2} \rangle \right]^2$$

$$W = \left[W(J_1 J_1 J_1 J_1 ; \nu J_o) \right]^2$$

with

$$0 \leq \nu \leq 2J_1$$

Moreover, if at the energies of this experiment only the elastic channel is supposed to be open, the Hauser-Feshbach penetrability term becomes

$$\tau = T_{\ell_1} (E_1)$$

The product NCW, in which appear terms indipendent of the energy and angle, can now be grouped into a single factor which can be tabulated, as reported in a previously mentioned work ([24]). Eq (1), then, becomes

$$\frac{d\delta}{d\Omega} = \frac{1}{8} \lambda^2 \Sigma_{i\nu} \alpha_{i\nu} \tau_i P_\nu (\cos\Theta)$$

The values of the coefficients $\alpha_{i\nu}$ for the transition $1^+ \rightarrow J_1 \pi_1 \rightarrow 1^+$ which have been used in the present work for calculating the angular distributions of the compound elastic scattering for ^{6}Li nucleus are listed in table 4. The values for the transition $0^+ \rightarrow J_1 \pi_1 \rightarrow 0^+$ for the ^{12}C necleus are listed in table 5.

TABLE 4 - $1^+ \rightarrow J_1\pi_1 \rightarrow 1^+$ transition sequence

ℓ_1	j_1	$J_1\pi_1$	ℓ_2	j_2	α_{i_0}	α_{i_2}	α_{i_4}
0	1/2	$1/2^+$	0	1/2	0,66667		
			2	3/2	0,66667		
		$3/2^+$	0	1/2	1,33333		
			2	3/2	1,33333		
				5/2	1,33333		
1	1/2	$1/2^-$	1	1/2	0,66667		
				3/2	0,66667		
		$3/2^-$	1	1/2	1,33333		
				3/2	1,33333		
			3	5/2	1,33333		
	3/2	$1/2^-$	1	1/2	0,66667		
				3/2	0,66667		
		$3/2^-$	1	1/2	1,33333		
				3/2	1,33333	0,05333	
			3	5/2	1,33333	0,21333	
		$5/2^-$	1	3/2	2,00000	1,12000	
			3	5/2	2,00000	1,05142	
				7/2	2,00000	1,42857	
2	3/2	$1/2^+$	0	1/2	0,66667		
			2	3/2	0,66667		
		$3/2^+$	0	1/2	1,33333		
			2	3/2	1,33333	0,05333	
				5/2	1,33333	0,21333	
		$5/2^+$	2	3/2	2,00000	1,12000	
				5/2	2,00000	1,05142	
			4	7/2	2,00000	1,42857	
	5/2	$3/2^+$	0	1/2	1,33333		
			2	3/2	1,33333	0,10666	
				5/2	1,33333	0,85248	
		$5/2^+$	2	3/2	2,00000	1,05142	
				5/2	2,00000	0,98705	0,03498
			4	7/2	2,00000	1,34110	-0,15473
		$7/2^+$	2	5/2	2,66667	2,33236	0,76967

%

×

ℓ_1	j_1	$J_1\pi_1$	ℓ_2	j_2	α_{i_0}	α_{i_2}	α_{i_4}
2	5/2	$7/2^+$	4	7/2	2,66667	2,20278	0,53644
				9/2	2,66667	2,53968	1,14285
3	5/2	$3/2^-$	1	1/2	1,33333		
				3/2	1,33333	0,10666	
			3	5/2	1,33333	0,85248	
		$5/2^-$	1	3/2	2,00000	1,05142	
			3	5/2	2,00000	0,98705	0,03498
				7/2	2,00000	1,34110	-0,15743
		$7/2^-$	3	5/2	2,66667	2,33236	0,76967
				7/2	2,66667	2,20278	0,53644
	7/2	$5/2^-$	1	3/2	2,00000	1,42857	
			3	5/2	2,00000	1,34110	-0,15743
				7/2	2,00000	1,82216	0,70845
		$7/2^-$	3	5/2	2,66667	2,21818	0,13994
				7/2	2,66667	2,08040	0,37388
		$9/2^-$	3	7/2	3,33333	3,39506	1,96970
4	7/2	$5/2^+$	2	3/2	2,00000	1,42857	
				5/2	2,00000	1,34110	-0,15743
			4	7/2	2,00000	1,82216	0,70845
		$7/2^+$	2	5/2	2,66667	2,21818	0,13994
			4	7/2	2,66667	2,08040	0,37388
				9/2	2,66667	2,39858	0,79654
		$9/2^+$	4	7/2	3,33333	3,39506	1,96970
				9/2	3,33333	3,25476	1,62534
	9/2	$7/2^+$	2	5/2	2,66667	2,53968	1,14285
			4	7/2	2,66667	2,39858	0,79654
				9/2	2,66667	2,76534	1,69696
		$9/2^+$	4	7/2	3,33333	3,25476	1,62534
				9/2	3,33333	3,13422	1,34119
		$11/2^+$	4	9/2	4,00000	4,37565	3,14581

TABLE 5 - $0^+ \rightarrow J_1 \pi_1 \rightarrow 0^+$ transition sequence

ℓ_1	j_1	$J_1 \pi_1$	ℓ_2	j_2	α_{i0}	α_{i2}	α_{i4}
0	1/2	$1/2^+$	0	1/2	2,00000		
1	1/2	$1/2^-$	1	1/2	2,00000		
	3/2	$3/2^-$	1	3/2	4,00000	4,00000	
2	3/2	$3/2^+$	2	3/2	4,00000	4,00000	
	5/2	$5/2^+$	2	5/2	6,00000	6,85714	5,14285
3	5/2	$5/2^-$	3	5/2	6,00000	6,85714	5,14285
	7/2	$7/2^-$	3	7/2	8,00000	9,52380	8,41558
4	7/2	$7/2^+$	4	7/2	8,00000	9,52380	8,41558
	9/2	$9/2^+$	4	9/2	10,00000	12,12121	11,32867

REFERENCES

(1) Cinda 72 - Int.Atomic Energy Agency,Vienna 1972.

(2) R. Batchelor and J.H. Towle - Nuclear Phys. 47 (1963) 385.

(3) J.C. Hopkins and D. Drake - Nuclear Phys. A107 (1968) 139.

(4) J.E. Wills, J.K. Bair, H.O. Cohn and H.B. Willard - Phys. Rew. 109 (1958) 891.

(5) R.O. Lane, A.S. Langsdorf Jr. J.E. Monahan and A.J. Elwin - Ann. of Phys. 12 (1961) 135.

(6) M. Walt and J.R. Bejster - Phys. Rew. 98 (1955) 677.

(7) Perey - ORNL 44441 nov. 1969.

(8) R. Budde and P. Huber - Hel. Phys. Acta 28 (1955) 49.

(9) S. Cierjaks, P. Forti, D. Kopsch, L. Kropp, J. Nebe and H. Unseld - KFK1000-EUR3963e-EANDC(E)-111"V" (1968).

(10) D. Lister and A. Sayres - Phys. Rew. 143 (1966) 745.

(11) A. Metellini - Univ. of Padua, Thesis (1970).

(12) D.W. Glasgow, D.G. Foster Jr.- Bull. Am. Phys. Soc. 8 (1963) 321 HW-73116 (1963); HW-77311 (1963).

(13) C.K. Bockelman, D.W. Miller, R.K. Adair and H.H. Barschall- Phys. Rew. 84 (1951) 69.

(14) P. Boschung, J.T. Lindow and E.F. Shrader - Nucl. Phys. A161 (1971) 593.

(15) M. Forte - Suppl. Nuovo Cimento 9 (1958) 390.

(16) V.V. Verbinski, W.R. Burrns, T.A. Love, W. Zobel, D.R. Nygren and C.D. Zafiratos - Nucl. Inst. Meth. 31 (1964) 226.

(17) J.E. Brolley Jr. and J.H. Fowler - Fast Neutron Phys.PartI- I.B.Marion and J.L. Fowler Ed. - Interscience Publishers, N.Y. (1960).

(18) S.T. Thornton - Nucl. Phys. A136 (1969) 25.

(19) F. Ajzenberg-Selov and T. Lauritsen - Nucl. Phys. 78 (1966) 1.

(20) C.M. Lederer, J.M. Hollander and I. Perlman - Table of Isotopes, VI Ed.-John Wiley and Sons Inc. N.Y. (1968).

(21) F.P. Agee and L. Rosen - Los Alamos Rep. L.A.- 3538-MS Vol.I (1966).

(22) L. Rosen and L. Stewart - Phys. Rew. 126 (1962) 1150.

(23) V. Benzi, F. Fabbri and A.M. Saruis - SMOG un programma peril calcolo dei parametri d'interazione neutrone--nucleo con il modello ottico-Unpublished.

(24) E. Sheldon and D.M. Van Patter - Rew. of Mod. Phys. 38 (1966) 143.

(25) F. Perey and B. Buck - Nucl. Phys. 32 (1962) 353.

(26) F. Demanins, G. Nardelli and G. Pauli - Report INFN/BE - 71/8 (1971).

(27) F. Ajzenberg-Selov - Nucl. Phys. A152 (1970) 17.

(28) R.B. Knowlen and A.A. O'Dell - Nucl. Inst. Meth. 78 (1970) 300.

(29) S.A. Cox - Nucl. Inst. Meth. 56 (1967) 245.

(30) W. Galati, J.D. Brandenberger and J.L. Weil - Phys. Rew. C 5 (1972) 1508.

* * *